Mixed Integer Linear Programming for Discrete Sampling Scheme Design in Diffusion MRI

Si-Miao Zhang[1], Jing Wang[1], Yi-Xuan Wang[1], Tao Liu[2], Haogang Zhu[1], Han Zhang[3,4], and Jian Cheng[1]

[1] State Key Laboratory of Complex & Critical Software Environment (CCSE), Beihang University, China
{haogangzhu,jian_cheng}@buaa.edu.cn
[2] School of Biological Science and Medical Engineering, Beihang University, China
[3] School of Biomedical Engineering & State Key Laboratory of Advanced Medical materials and Devices, ShanghaiTech University, China
[4] Shanghai Clinical Research and Trial Center, China

Abstract. In diffusion MRI (dMRI), a uniform single or multiple shell sampling scheme is typically required for data acquisition in **q**-space, because uniform spherical sampling offers the advantage of capturing more information using fewer samples, leading to superior reconstruction results. Uniform sampling problems can be categorized into continuous and discrete types. While most existing sampling methods focus on the continuous problem that is to design spherical samples continuously from single or multiple shells, this paper primarily investigates two discrete optimization problems, i.e., 1) optimizing the polarity of an existing scheme (P-P), and 2) optimizing the ordering of an existing scheme (P-O). Existing approaches for these two problems mainly rely on greedy algorithms, simulated annealing, and exhaustive search, which fail to obtain global optima within a reasonable timeframe. We propose several Mixed Integer Linear Programming (MILP) based methods to address these problems. To the best of our knowledge, this is the first work that solves these two discrete problems using MILP to obtain global optimal or sufficiently good solutions in 10 minutes. Experiments performed on single and multiple shells demonstrate that our MILP methods can achieve larger separation angles and lower electrostatic energy, resulting better reconstruction results, compared with existing approaches in commonly used software (i.e., CAMINO and MRtrix).

Keywords: Diffusion MRI · Signal Sampling · Signal Reconstruction · Mixed Integer Linear Programming.

1 Introduction

Diffusion MRI (dMRI) is a unique technique to non-invasively study microstructural tissue properties of white matter and reconstruct fiber tracts in the human brain. In dMRI, diffusion weighted imaging (DWI) data is typically acquired using a single or multiple shell sampling scheme in **q**-space (i.e, the 3D acquisition

parameter space of b value and b vector). Subsequently, the acquired DWI data is fitted using various diffusion models, including Diffusion Tensor Imaging (DTI) model [1] and various High Angular Resolution Diffusion Imaging (HARDI) models [14,3,12,15]. Diffusion models provide important diffusion quantities to reveal various tissue properties, including fractional anisotropy (FA), generalized FA (GFA), fiber Orientation Distribution Function (fODF), etc. The quality of reconstruction results is directly influenced by quality of sampling schemes. Thus designing an appropriate sampling scheme is highly necessary.

Without any prior knowledge of fiber orientations, a good sampling scheme requires signal samples to be uniformly distributed in sphere. A large angular separation between samples results in a large angular resolution and ensures good rotational invariance in reconstruction [4]. Uniform sampling problems can be categorized into continuous and discrete types. Most existing sampling methods address the continuous problem, which aims to design a uniform single/multiple shell sampling scheme in the continuous sphere $\mathbb{S}^2$. Electrostatic Energy Minimization (EEM) [10,2] designs sampling schemes by minimizing electrostatic energy, which has been used in Human Connectome Project (HCP) [11]. While Spherical Code (SC) [4] method directly maximizes the minimal angular separation between samples (i.e., covering radius, which is defined as $d(\{\mathbf{u}_i\}_{i=1}^N) = \min_{i \neq j} \arccos(\mathbf{u}_i^T \mathbf{u}_j)$ for a given sample set $\{\mathbf{u}_i\}_{i=1}^N$). Bases on an existing scheme acquired by continuous sampling optimization, discrete problems aim at further optimize a subsampling set [2], the ordering [6,7], and the polarity [13] of the existing scheme. In this paper, we mainly address two of the discrete problems mentioned above, i.e., 1) optimizing the polarity of an existing scheme (P-P), and 2) optimizing the ordering of an existing scheme (P-O).

Optimizing the polarity of an existing scheme (P-P) proves valuable for eddy current correction [1]. Sampling scheme design in dMRI normally requires the antipodal symmetry constraint (i.e., a sample $\mathbf{u}$ is equivalent to its negative $-\mathbf{u}$). However, for effective eddy current correction, it becomes necessary to optimize the polarity, i.e., the signs of directions, of a given scheme. This optimization ensures that the scheme, with its adjusted polarity, remains uniform without the antipodal symmetry constraint. Consequently, the samples should be distributed across the entire sphere rather than being confined to a hemisphere. `dirflip` in MRtrix [2] employs brute-force random search to optimize polarity for the single shell case (P-P-S).

Optimization of the ordering of an existing scheme (P-O) is crucial, particularly in scenarios involving potential scan interruptions. Premature termination of a scan may result in a non-uniform partial scan, thereby compromising the quality of reconstruction outcomes. Scanning infants or patients with epilepsy, for example, is especially troublesome because they are incapable of staying still during the long scanning time. Dubois *et al.* [8] proposed to separate close gradient directions into different subsets to gain better partial scans. Cook *et al.* [6] proposed using simulated annealing to optimize a weighted average of elec-

[1] `https://fsl.fmrib.ox.ac.uk/fsl/fslwiki/eddy`

[2] `https://mrtrix.readthedocs.io/en/dev/reference/commands/dirflip.html`

trostatic energies of all partial subsets, which was released as `orderpoints` in CAMINO [3]. `dirorder` in MRtrix [13] [4] implements a greedy incremental EEM (IEEM) method for single shell case (P-O-S) [7,2].

Existing methods (CAMINO [6] and MRtrix [13]) mainly focus on single shell case for P-P and P-O, and fail to obtain global optima within a reasonable timeframe. Moreover, simulated annealing and brute-force exhaustive search are known to be computationally inefficient. In this paper, we propose novel Mixed Integer Linear Programming (MILP) methods for these two discrete sampling scheme design problems in both single and multiple shell cases. Experiment results show that MILP can archive larger angular separation and lower electrostatic energy, compared with existing methods in CAMINO [6] and MRtrix [13].

2 Methods

2.1 Optimize the polarity of a scheme (P-P)

The P-P-S problem is to minimize the electrostatic energy of a given single shell scheme $\{\mathbf{u}_i\}_{i=1}^N$ by flipping certain points on the sphere, i.e.,

$$\min_{h_i\in\{-1,1\}} E(\{h_i\mathbf{u}_i\}_{i=1}^N), \quad \text{where } E(\{\mathbf{v}_i\}_{i=1}^N) = \sum_{i\neq j}\frac{1}{\|\mathbf{v}_i-\mathbf{v}_j\|^2} \tag{1}$$

where $E(\{\mathbf{v}_i\}_{i=1}^N)$ is the electrostatic energy of $\{\mathbf{v}_i\}_{i=1}^N$. We propose Mixed Integer Linear Programming (MILP) to solve Eq. (2) as follows:

$$\min_{\{h_i\},\{x_{i,j}\}} \sum_{i<j}\left((1-x_{i,j})\frac{1}{\|\mathbf{u}_i-\mathbf{u}_j\|^2}+x_{i,j}\frac{1}{\|\mathbf{u}_i+\mathbf{u}_j\|^2}\right) \tag{2a}$$

$$s.t.\ h_i = 0,1, \quad \forall i \tag{2b}$$

$$x_{i,j} \le h_i + h_j, \quad x_{i,j} \le 2 - h_i - h_j, \quad \forall i,j \tag{2c}$$

$$x_{i,j} \ge h_i - h_j, \quad x_{i,j} \ge h_j - h_i, \quad \forall i,j, \tag{2d}$$

where $h_i = 0,1$ indicates whether or not to flip the i-th sample, and $x_{i,j}$ is constrained to represent h_i xor h_j. Thus, Eq. (2a) is the flipped energy if exactly one of the two samples flipped ($x_{i,j}=1$), and it chooses the original energy otherwise ($x_{i,j}=0$). Similarly, the multi-shell case P-P-M can be formulated as

$$\begin{aligned}\min_{\{h_{s,i}\},\{x_{s,i,t,j}\}} & wS^{-1}\sum_{s=1}^{S}\frac{1}{N_s^2}\sum_{i<j}\left(\frac{1-x_{s,i,s,j}}{\|\mathbf{u}_{s,i}-\mathbf{u}_{s,j}\|^2}+\frac{x_{s,i,s,j}}{\|\mathbf{u}_{s,i}+\mathbf{u}_{s,j}\|^2}\right)\\ &+(1-w)\frac{1}{N^2}\sum_{s\neq t}\sum_{i=1}^{N_s}\sum_{j=1}^{N_t}\left(\frac{1-x_{s,i,t,j}}{\|\mathbf{u}_{s,i}-\mathbf{u}_{t,j}\|^2}+\frac{x_{s,i,t,j}}{\|\mathbf{u}_{s,i}+\mathbf{u}_{t,j}\|^2}\right)\end{aligned} \tag{3a}$$

$$s.t.\ h_{s,i} = 0,1, \quad \forall s,i \tag{3b}$$

$$x_{s,i,t,j} \le h_{s,i} + h_{t,j}, \quad x_{s,i,t,j} \le 2 - h_{s,i} - h_{t,j}, \quad \forall s,i,t,j \tag{3c}$$

$$x_{s,i,t,j} \ge h_{s,i} - h_{t,j}, \quad x_{s,i,t,j} \ge h_{t,j} - h_{s,i}, \quad \forall s,i,t,j \tag{3d}$$

[3] `http://camino.cs.ucl.ac.uk/index.php?n=Man.Orderpoints`

[4] `https://mrtrix.readthedocs.io/en/dev/reference/commands/dirorder.html`

where $h_{s,i}$ indicates whether or not to flip the i-th sample on the s-th shell. MILP can be solved using branch and cut method. We adopt GULOBI [9] to solve Eq. (2) and Eq. (3), which can provide a global solution or a reasonably optimized solution within minutes. In practice, we adopt results of GUROBi after optimizing for 10 minutes, which already provides good performance.

2.2 Optimize the ordering of a scheme (P-O)

Global Optimization. Given a scheme $\{\mathbf{u}_i\}_{i=1}^N$, P-O is to optimize its ordering to obtain a permuted scheme $\{\mathbf{u}_{\sigma_i}\}_{i=1}^N$, such that it maximizes angular separation for every partial subset $\{\mathbf{u}_{\sigma_1}, \ldots, \mathbf{u}_{\sigma_k}\}$, $2 \leq k \leq N$. However, smaller number of samples in a subset indicates larger covering radius, which results in difficulty to design the weights. To avoid this issue, we design a loss function based on spherical packing density [5], which normally does not change a lot with the number of samples. Spherical packing density measures the fraction of spherical space occupied by a given spherical packing. For a given subset $\{\mathbf{u}_{\sigma_1}, \ldots, \mathbf{u}_{\sigma_k}\}$ with covering radius $\theta_k = d(\{\mathbf{u}_{\sigma_i}\}_{i=1}^k)$, its packing density is $\frac{2\pi(1-\cos\frac{\theta_k}{2})2k}{4\pi} = (1-\cos\frac{\theta_k}{2})k = (1-\sqrt{\frac{\cos\theta_k+1}{2}})k \approx (1-\frac{\cos\theta_k+1}{2})k = \frac{1-\cos\theta_k}{2}k$. For single shell case P-O-S, we optimize the sum of approximated packing densities as

$$\max_{\{\theta_k\},\{x_{i,j}\}} \sum_{k=2}^{N} \frac{1-\cos\theta_k}{2}k \tag{4a}$$

$$s.t.\ \cos\theta_k \geq |\mathbf{u}_i^T\mathbf{u}_j| - (2 - \sum_{m=1}^{k} x_{i,m} - \sum_{m=1}^{k} x_{j,m})M,\ \forall i<j, \forall 2 \leq k \leq N \tag{4b}$$

$$\sum_{i=1}^{N} x_{i,j} = 1, \forall j, \quad \sum_{j=1}^{N} x_{i,j} = 1, \forall i, \quad x_{i,j} = 0, 1, \forall i, j \tag{4c}$$

where $x_{i,j} = 1$ indicates $\mathbf{u}_i$ being ordered to the j-th position in the new scheme, i.e., $\sigma_j = i$, and Eq. (4c) ensures that $\{\sigma_j\}$ is indeed a permutation. In Eq. (4b), $\sum_{m=1}^{k} x_{i,m}$ equals 1 if the $\mathbf{u}_i$ is chosen as one of the first k samples in the new scheme, and it is 0 otherwise. Thus, the constraint Eq. (4b) only takes effect if and only if both $\mathbf{u}_i$ and $\mathbf{u}_j$ are chosen among the first k samples. Eq. (4) is an MILP problem, when considering $\cos\theta_k$ as a variable.

Similarly, we design a weighted mean of approximated packing densities for multi-shell case P-O-M. Given N_s samples $\{\mathbf{u}_{s,i}\}_{i=1}^{N_s}$ in S shells, $s = 1, 2, \ldots S$, we stack them together with the ordering $\{\mathbf{u}_i\}_{i=1}^N, N = \sum_{s=1}^{S} N_s$, and use I_s to

[5] `https://en.wikipedia.org/wiki/Packing_density`

represent the s-th shell's index set. Then, an MILP problem is formulated as

$$\max_{\{\theta_{s,k}\},\{x_{i,j}\}} wS^{-1}\sum_{s=1}^{S}\frac{N_s}{N}\sum_{k=2}^{N}\frac{1-\cos\theta_{s,k}}{2}k+(1-w)\sum_{k=2}^{N}\frac{1-\cos\theta_{0,k}}{2}k \tag{5a}$$

$$s.t.\ \cos\theta_{0,k}\geq|\mathbf{u}_i^T\mathbf{u}_j|-(2-\sum_{m=1}^{k}x_{i,m}-\sum_{m=1}^{k}x_{j,m})M,\ \forall i<j,\forall k \tag{5b}$$

$$\cos\theta_{s,k}\geq|\mathbf{u}_i^T\mathbf{u}_j|-(2-\sum_{m=1}^{k}x_{i,m}-\sum_{m=1}^{k}x_{j,m})M,\ \forall i,j\in I_s,\forall k,\forall s \tag{5c}$$

$$\sum_{i=1}^{N}x_{i,j}=1,\forall j,\quad \sum_{j=1}^{N}x_{i,j}=1,\forall i,\quad x_{i,j}=0,1,\forall i,j, \tag{5d}$$

where $\theta_{0,k}$ is the covering radius of the first k samples, and $\theta_{s,k}$ is the covering radius of the s-th shell among the first k samples.

Incremental Optimization. Eq. (4) has $O(K^3)$ numbers of constrains and is computationally inefficient for problems with large sizes. Thus, we propose an incremental optimization way to divide the entire task into sequences and solve them one by one. The incremental optimization is: assuming we have already optimized the first m orders $\{\mathbf{u}_1,\ldots,\mathbf{u}_m\}$, we pick the next p samples from the rest $N-m$ samples and sort them to achieve maximum loss function.

$$\max_{\{\theta_k\},\{x_{i,j}\}}\sum_{k=m+1}^{m+p}\frac{1-\cos\theta_k}{2}k \tag{6a}$$

$$s.t.\ \cos\theta_k\geq|\mathbf{u}_i^T\mathbf{u}_j|-(2-\sum_{l=m+1}^{k}x_{i,l}-\sum_{l=m+1}^{k}x_{j,l})M,\ \forall m+1\leq i<j,\forall k \tag{6b}$$

$$\cos\theta_k\geq|\mathbf{u}_i^T\mathbf{u}_j|-(1-\sum_{l=m+1}^{k}x_{i,l})M,\ \forall j\leq m<i,\forall k \tag{6c}$$

$$\cos\theta_k\geq|\mathbf{u}_i^T\mathbf{u}_j|,\ \forall 1\leq i<j\leq m,\forall m+1\leq k\leq m+p \tag{6d}$$

$$\sum_{i=m+1}^{N}x_{i,j}=1,\ \forall m+1\leq j\leq m+p,\quad \sum_{j=m+1}^{m+p}x_{i,j}\leq 1,\ \forall m+1\leq i\leq N \tag{6e}$$

$$x_{i,j}=0,1,\ \forall m+1\leq i\leq N,\forall m+1\leq j\leq m+p, \tag{6f}$$

where covering radius θ_k is constrained by newly added points in (6b), by fixed points and newly added points in Eq. (6c), and by fixed points in Eq. (6d).

Similarly to Eq. (5), an MILP for the multi-shell case P-O-M is

$$\max_{\{\theta_{s,k}\},\{x_{i,j}\}} wS^{-1}\sum_{s=1}^{S}\frac{N_s}{N}\sum_{k=m+1}^{m+p}\frac{1-\cos\theta_{s,k}}{2}k+(1-w)\sum_{k=m+1}^{m+p}\frac{1-\cos\theta_{0,k}}{2}k \quad (7a)$$

$$s.t.\ \cos\theta_{0,k}\geq|\mathbf{u}_i^T\mathbf{u}_j|-(2-\sum_{l=m+1}^{k}x_{i,l}-\sum_{l=m+1}^{k}x_{j,l})M,\ \forall m<i<j,\forall k \quad (7b)$$

$$\cos\theta_{s,k}\geq|\mathbf{u}_i^T\mathbf{u}_j|-(2-\sum_{l=m+1}^{k}x_{i,l}-\sum_{l=m+1}^{k}x_{j,l})M,\ \forall m<i<j,i,j\in I_s,\forall k \quad (7c)$$

$$\cos\theta_{0,k}\geq|\mathbf{u}_i^T\mathbf{u}_j|-(1-\sum_{l=m+1}^{k}x_{i,l})M,\ \forall j\leq m<i,\forall k \quad (7d)$$

$$\cos\theta_{s,k}\geq|\mathbf{u}_i^T\mathbf{u}_j|-(1-\sum_{l=m+1}^{k}x_{i,l})M,\ \forall j\leq m<i,i,j\in I_s,\forall k \quad (7e)$$

$$\cos\theta_{0,k}\geq|\mathbf{u}_i^T\mathbf{u}_j|,\ \forall 1\leq i<j\leq m,\forall m+1\leq k\leq m+p \quad (7f)$$

$$\cos\theta_{s,k}\geq|\mathbf{u}_i^T\mathbf{u}_j|,\ \forall 1\leq i<j\leq m,i,j\in I_s,\forall m+1\leq k\leq m+p \quad (7g)$$

$$\sum_{i=m+1}^{N}x_{i,j}=1,\ \forall m+1\leq j\leq m+p,\quad \sum_{j=m+1}^{m+p}x_{i,j}\leq 1,\ \forall m+1\leq i\leq N \quad (7h)$$

$$x_{i,j}=0,1,\ \forall m+1\leq i\leq n,\forall m+1\leq j\leq m+p. \quad (7i)$$

For the incremental optimization, we use MILP in Eq. (6) and Eq. (7) incrementally to optimize the ordering for every p samples. In the k-th step, we fix previous determined $(k-1)p$ samples, and pick the ordering of the next p samples from rest $N-(k-1)p$ points.

Greedy ordering. Following the incremental strategy in Incremental EEM (IEEM) [7] and Incremental generalized EEM (IGEEM) [2], which optimize electrostatic energy, we propose a similar incremental greedy algorithm for P-O to optimize covering radius and covering density. In the k-th step, with fixed $k-1$ previous determined samples, we choose the k-th sample from the rest $N-k$ samples to be the best one that optimizes the loss function (using covering radius or covering density) with existing $k-1$ points. We also add an extra step to iterate through the point set to determine the first point chosen. Note that the greedy method is just a special case of the incremental optimization method, when we set $p=1$ in Eq. (6). Thus, we could set the greedy optimization solution as the initial ordering in the incremental optimization.

3 Experiments

3.1 Evaluation on P-P

For the problem P-P, we compare the proposed MILP method (called MILP-P-S) with `dirflip` command from MRtrix on P-P-S. The experiment is evaluated

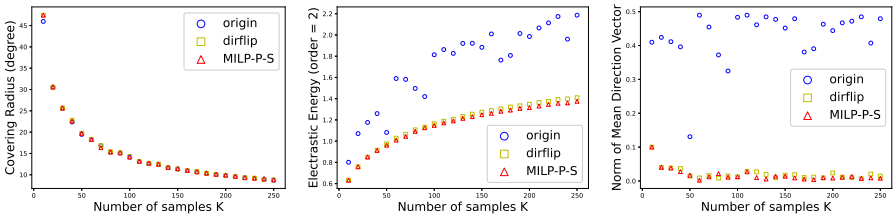

Fig. 1: **Optimization of Polarity (P-P-S)**. Comparison between `dirflip` and the proposed MILP-P-S on single shell ElectricRepusion dataset. Left: covering radius. Middle: electrostatic energy. Right: norm of mean direction vector.

Table 1: Optimization of Polarity (P-P-M).

	shell1		shell2		shell3		combine	
	radius	energy	radius	energy	radius	energy	radius	energy
Original HCP Scheme	10.79	1.285	10.34	1.215	10.73	1.231	2.381	1.743
`dirflip`	11.98	1.142	11.49	1.148	12.01	1.145	2.379	1.769
MILP-P-S	**12.01**	**1.122**	**12.51**	**1.116**	**12.33**	**1.111**	2.381	1.687
MILP-P-M	10.79	1.131	10.34	1.152	11.31	1.146	**4.569**	**1.408**

on ElectricRepusion dataset from CAMINO [5], which collects the best known single shell sampling schemes using EEM. MILP-P-S can give globally optimal result for schemes with no more than 26 points within 1 minutes and for schemes with no more than 32 points within 10 minutes. Fig. 1 demonstrates the results of covering radius, electrostatic energy which is the optimization goal of both methods, and norm of mean direction vector which serves as an indicator for asymmetry in `dirstat` command from MRtrix.

The multi-shell scheme with 90×3 samples in HCP is used to evaluate methods for the multi-shell problem P-P-M. `dirflip` in MRtrix cannot deal with P-P-M, because it does not consider relationship among shells. Our method MILP has the advantage of being possible to optimize three shells individually (MILP-P-S in Eq. (2)) and as a whole (MILP-P-M in Eq. (3)). Thus, we use MILP-P-M to optimize multiple shells, and use MILP-P-S and `dirflip` to optimize three shells individually. As shown in Table 1, MILP-P-S has larger angular separation and smaller electrostatic energy for individual single shells, while MILP-P-M results in a more uniform scheme in the combined shell.

3.2 Evaluation on P-O

For P-O-S, we compare `orderpoints` from camino, `dirorder` from MRtrix, and our MILP approach (called MILP-O-S). MILP-O-S in Eq. (4) has the potential to obtain global optimal ordering solution when the problem size is small. For sampling scheme with no more than 12 samples, MILP-O-S can obtain the global optima within 5 minutes, while `orderpoints` can run for hours without converging, and `dirorder` uses a greedy algorithm which cannot solve P-O-S

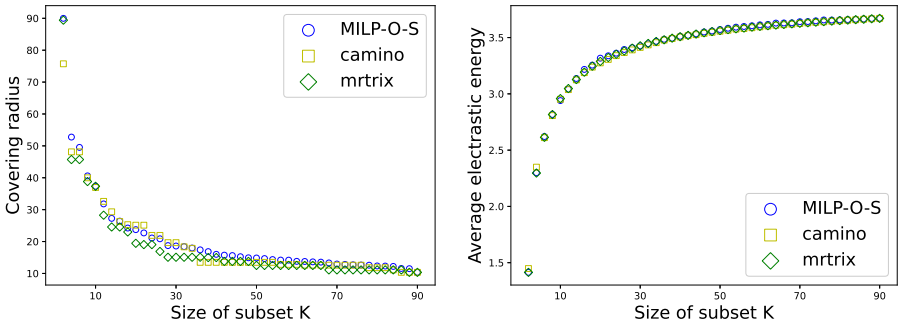

Fig. 2: **Optimization of Ordering (P-O-S)**.

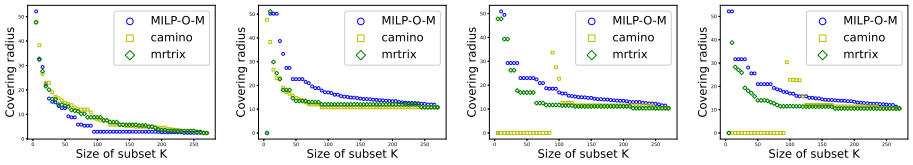

(a) Combined shell (b) Shell 1 (c) Shell 2 (d) Shell 3

Fig. 3: **Optimization of Ordering (P-O-M)**.

globally. We compare MILP-O-S to `orderpoints` on the second shell ($b = 2000$ s/mm^2) of the multi-shell HCP scheme in Fig. 2. The left part of Fig. 2 shows that MILP-O-S achieves largest separation angles, and the right part of Fig. 2 shows that MILP-O-S has near optimal electrostatic energies.

For P-O-M, we use the multi-shell HCP scheme with 90×3 samples for experiments. Since both `orderpoints` and `dirorder` are incapable of taking multiple shells into consideration. we apply these two methods to the combined shell with all 270 samples. Our MILP-O-M in Eq. (7) can naturally deal with multiple shell scenario. From the result in Fig. 3, since `orderpoints` and `dirorder` can only consider the combined shell, they outperform MILP-O-M in combined shell. However MILP can consider all shells simultaneously and performs significantly better than other methods in individual shells. Moreover, `orderpoints` only chooses the first 59 samples all from the first shell, which is not an acceptable multi-shell sampling ordering for reconstruction.

We perform non-negative spherical deconvolution (NNSD) [3] to evaluate the reconstructed fODFs and their peaks for P-M-O. The spherical harmonic order is set as 8. We evaluate the effect of ordering by choosing the first 60 samples from ordering of 90×3 samples as an illustration of scan interruption. Three partially scanned schemes with 60 samples from MILP-O-M, `orderpoints` and `dirorder` are evaluated. We display the resulting fODF fields together with detected peaks and with GFA images as backgrounds in Fig. 4 . Peaks are detected from the fODFs with GFA higher than 0.3. As can be seen in Fig. 4, both `orderpoints` and

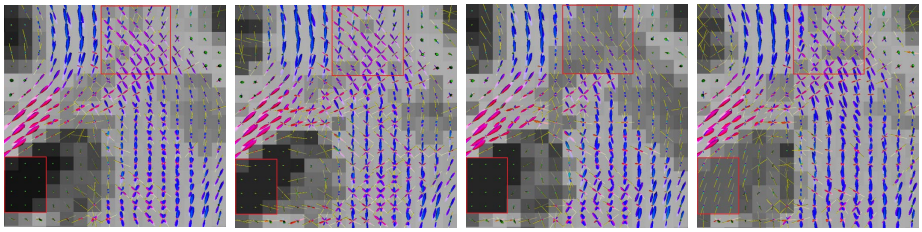

(a) Full scheme (b) MILP-O-M (c) CAMINO (d) MRtrix

Fig. 4: **Comparison of reconstruction results using partial scan data**.

`dirorder` have obvious flaw while our MILP-O-M yields the best reconstruction result, closer to the results by using full sampled data.

4 Conclusion

To the best of our knowledge, this is the first work to optimize the polarity and the ordering of an existing single or multi-shell sampling scheme using Mixed Integer Linear Programming (MILP). The proposed MILP formulations could obtain global optimal solutions for problems with small sizes, or sufficiently good solutions in 10 minutes. Experiments demonstrate that our proposed MILP methods achieves larger separation angles and lower electrostatic energy in single and multiple shell cases, resulting better reconstruction results, compared with existing approaches in commonly used software (i.e., CAMINO and MRtrix).

Acknowledgments. This work is partially supported by the STI 2030-Major Projects (No. 2022ZD0209000) and the National Natural Science Foundation of China (No. 61971017).

Disclosure of Interests. The authors have no competing interests to declare that are relevant to the content of this article.

References

1. Basser, P., Mattiello, J., LeBihan, D.: Mr diffusion tensor spectroscopy and imaging. Biophysical Journal **66**(1), 259–267 (1994)
2. Caruyer, E., Cheng, J., Lenglet, C., Sapiro, G., Jiang, T., Deriche, R.: Optimal Design of Multiple Q-shells experiments for Diffusion MRI. In: MICCAI Workshop on Computational Diffusion MRI (CDMRI'11). pp. 45–53 (2011)
3. Cheng, J., Deriche, R., Jiang, T., Shen, D., Yap, P.T.: Non-Negative Spherical Deconvolution (NNSD) for estimation of fiber Orientation Distribution Function in single-/multi-shell diffusion MRI. NeuroImage **101**, 750–764 (2014)
4. Cheng, J., Shen, D., Yap, P.T., Basser, P.J.: Single-and multiple-shell uniform sampling schemes for diffusion mri using spherical codes. IEEE transactions on medical imaging **37**(1), 185–199 (2017)

5. Cook, P., Bai, Y., Nedjati-Gilani, S., Seunarine, K., Hall, M., Parker, G., Alexander, D.: Camino: Open-source diffusion-mri reconstruction and processing. Proc. Intl. Soc. Magn. Reson. Med. **14** (11 2005)
6. Cook, P.A., Symms, M., Boulby, P.A., Alexander, D.C.: Optimal acquisition orders of diffusion-weighted mri measurements. Journal of Magnetic Resonance Imaging **25**(5), 1051–1058 (2007)
7. Deriche, R., Calder, J., Descoteaux, M.: Optimal real-time q-ball imaging using regularized kalman filtering with incremental orientation sets. Medical Image Anal. **13**(4), 564–579 (2009)
8. Dubois, J., Poupon, C., Cointepas, Y., Lethimonnier, F., Bihan, D.: Diffusion gradient orientation schemes for dti acquisitions with unquiet subjects (01 2004)
9. Gurobi Optimization, LLC: Gurobi Optimizer Reference Manual (2023), `https://www.gurobi.com`
10. Jones, D., Horsfield, M., Simmons, A.: Optimal strategies for measuring diffusion in anisotropic systems by magnetic resonance imaging. Magnetic resonance in medicine **42**(3), 515–525 (September 1999)
11. Sotiropoulos, S.N., Jbabdi, S., Xu, J., Andersson, J.L.R., Moeller, S., Auerbach, E.J., Glasser, M.F., Hernández, M., Sapiro, G., Jenkinson, M., Feinberg, D.A., Yacoub, E., Lenglet, C., Essen, D.C.V., Ugurbil, K., Behrens, T.E.J.: Advances in diffusion MRI acquisition and processing in the human connectome project. NeuroImage **80**, 125–143 (2013)
12. Tournier, J.D., Calamante, F., Connelly, A.: Robust determination of the fibre orientation distribution in diffusion MRI: non-negativity constrained super-resolved spherical deconvolution. NeuroImage **35**(4), 1459–1472 (2007)
13. Tournier, J.D., Smith, R., Raffelt, D., Tabbara, R., Dhollander, T., Pietsch, M., Christiaens, D., Jeurissen, B., Yeh, C.H., Connelly, A.: Mrtrix3: A fast, flexible and open software framework for medical image processing and visualisation. NeuroImage **202**, 116137 (2019)
14. Tuch, D.S., Reese, T.G., Wiegell, M.R., Makris, N., Belliveau, J.W., Wedeen, V.J.: High angular resolution diffusion imaging reveals intravoxel white matter fiber heterogeneity. Magnetic Resonance in Medicine **48**(4), 577–582
15. Zhang, H., Schneider, T., Wheeler-Kingshott, C.A., Alexander, D.C.: Noddi: practical in vivo neurite orientation dispersion and density imaging of the human brain. Neuroimage **61**(4), 1000–1016 (2012)